THEORETICAL CONDITIONS RELATED TO AN OPEN CHANNEL FLOW LINEAR TURBINE

K. Ishida, Professor and M. J. Service, Lecturer, MNZIE

Faculty of Engineering

Fukui Institute of Technology

Fukui, Japan

ABSTRACT

The flow conditions related to a cascade of vanes supported on cables and moving in a continuous horizontal loop transverse to an open channel flow, are analysed. The energy and continuity equations for open channel flow are used to relate flow conditions upstream and downstream of the vanes and the Euler turbine equation is used to express the energy transfer from the flow to the vanes. Values for the force on a cascade of vanes set at various angles and depths in an open channel flow are calculated by the theory and found to show reasonable agreement with experimental results. The theoretical performance of a two stage linear turbine is calculated over a range of vane speeds and the maximum theoretical output determined.

NOMENCLATURE

C = average flow velocity
E = specific energy
F = force
g = gravitational constant
h = depth of flow
k = function of β and q
P = power per unit width of upstream flow
q = flow per unit width of upstream flow
Q = volume rate of flow
S = vane spacing
U = vane speed
V = average flow velocity relative to vanes
w = vane channel width
α = average flow angle to direction at right angles to direction of U (+ve when C_t in direction of U)
β = angle of relative flow velocity to direction at right angles to direction of U (+ve when V_t in direction of U)
ρ = density of flow

Subscripts

1 = stage 1
2 = stage 2
c = critical flow conditions
i = conditions at inlet to vane channel
o = conditions at outlet to vane channel
t = velocity component in direction transverse to upstream flow
max = maximum value
min = minimum value

INTRODUCTION

The system discussed in this paper is called a linear turbine due to its similarity to an axial flow turbine of infinite rotor diameter. It consists of a cascade arrangement of vanes supported on cables and moving in a continuous horizontal loop transverse to an open channel flow.

Interest in this type of system arises from the need, especially in developing countries, for a simple, inexpensive means of harnessing the seasonal low head energy potential of rivers and canals. The open channel flow linear turbine is well suited to this application since, due to low flow loadings and simple design, it can be constructed from inexpensive, locally available materials such as wood, bamboo, rope, etc., using local manpower. Also since its configuration allows for simple length adjustment to suit river width, and does not require extensive site preparation, it can be easily relocated and modified to suit seasonal flow conditions.

The principle of the linear turbine is similar to that of the tracked vehicle system studied by Powe [1], the lift translator system of Schneider [2], and the free wing turbine system of Goggins [3]. However, in all these systems the vanes are completely immersed in the working fluid (air or water) and design conditions can be approximated by airfoil theory and axial flow turbine theory, with axial velocity assumed to remain constant. With the open channel flow system considered in this paper the flow depth and axial velocity vary continuously from upstream to downstream and are governed by open channel flow conditions, hence analysis of the flow conditions involves a combination of open channel flow theory and axial flow turbine theory.

To date the authors have been unable to locate any design data covering these conditions and this paper is an attempt at developing a basic theory to enable an assessment of the feasibility of a linear turbine system for application to rivers, canals, etc. .

PRINCIPLE AND LAYOUT

The layout of the linear turbine is shown in Fig. 1. The two continuous loop cables pass around wheels at each end and support the vanes which are immersed in the channel flow. Due to the angle of the vanes the flow is obstructed and deflected causing an increase in depth upstream of the vanes and a reaction force on the vanes. This force is restrained by the tension in the supporting cables and the transverse component rotates the wheels which are used to drive either a generator for electricity or a pump for irrigation. On passing around the wheels the vanes swing freely to take up the opposite attitude to the flow, thus providing a further positive driving force in the opposite direction.

The energy available to the system is the difference in energy between the upstream and downstream flows and theoretically the greater the obstruction to the flow, and hence deeper the upstream flow, the greater the energy available. In practice however this will depend on the strength of the turbine components and the allowable increase in river depth at the site.

For maximum utilization of the available energy, the flow immediately downstream of the vanes should have minimum energy. This condition corresponds to critical flow which is the conditioning pertaining to uniform flow in open channels.

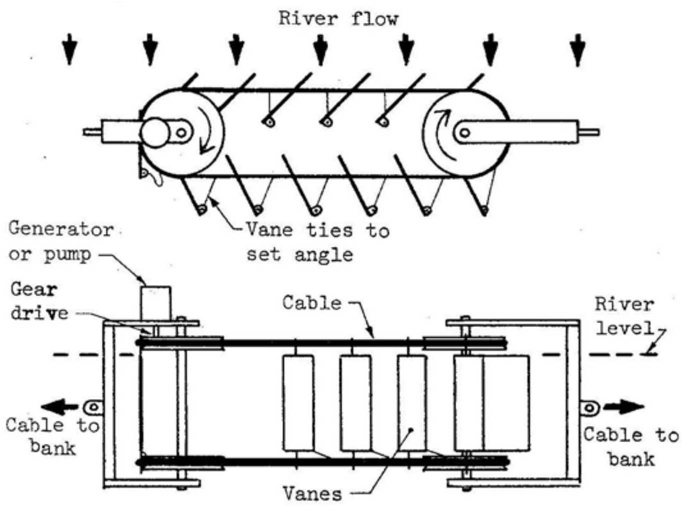

Fig.1 Layout of the linear turbine

CHANNEL FLOW

To analyse the system the flow conditions upstream, through the vanes, and downstream must be determined. As a first approximation these conditions can be considered similar to those of in viscid open channel flow in a rectangular channel for which the energy equation can be written as [4]:

$$E = C^2 / 2g + h \tag{1}$$

and the continuity equation as:

$$q = C \times h \tag{2}$$

The conditions for critical flow (minimum flow energy) can be found by differentiating the energy equation with respect to h and equating to zero. The critical depth and velocity can then be expressed as:

$$h_c = (q^2 / g)^{1/3} \;\; ; \; C_c = (gh_c)^{1/2} \tag{3}$$

and in terms of the minimum energy:

$$h_c = \frac{2}{3} E_{\min} \;\; ; \; C_c^2 / 2g = \frac{1}{3} E_{\min} \tag{4}$$

<u>Available energy</u>. Based on these expressions for channel flow the energy available to the turbine is:

$E_{available}$ = upstream flow energy – downstream flow energy for critical flow

$$= C_i^2 / 2g + h_i - E_{\min} \tag{5}$$

Maximum utilization of this energy requires flow deflection, by the upstream and downstream vanes, and flow velocities to be at optimum values. Flow deflection and velocity however are limited by conditions for critical flow in the vane channels.

<u>Critical flow width</u>. For in viscid flow the energy of the relative flow through the vane channels can be considered constant. The energy equation for this flow can be written as:

$$E = \frac{1}{2g} (Q / wh)^2 + h \;\; ; \; (V = Q / wh) \tag{6}$$

$$w = Q / (h (2g (E - h))^{1/2}) \tag{7}$$

Graphs of h and V versus w for constant Q and E are given in Fig. 2. These figures show that for constant Q and E there is a minimum flow width. At this minimum width the depth and velocity correspond to the critical depth h_c and critical velocity V_c. Any further reduction in width results in a reduction in flow.

For subcritical flows, decreasing the width results in a reduction in depth and increase in velocity. For supercritical flows, decreasing the width results in an increase in depth and a decrease in velocity. This situation is similar to that found in gas dynamics with flow through a nozzle, supercritical and subcritical corresponding to supersonic and subsonic respectively. In nozzle flow the critical flow width (or area) produces choked flow with sonic velocity.

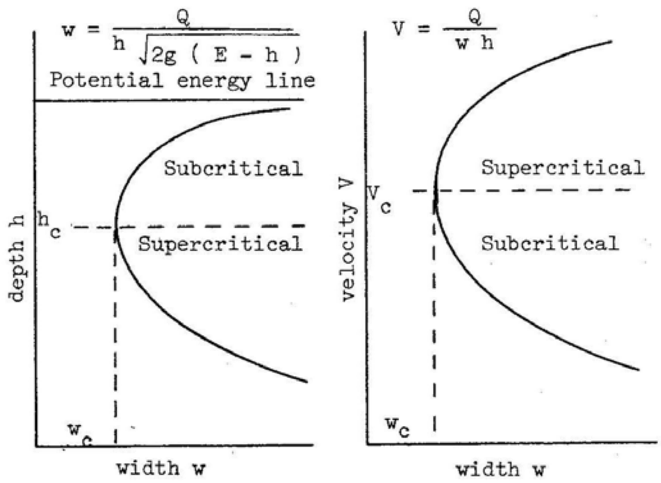

Fig. 2 Variation of flow depth and velocity with width (E and Q constant)

(a) Vane channel width and vane angle

(b) Critical vane speed

Fig. 3 Critical vane angle and speed

<u>Critical vane angles</u>. The flow width through the vanes depends upon the vane outlet angle β_o as shown in Fig. 3a. This relationship can be written as:

$$w = S\cos\beta_o \tag{8}$$

For critical conditions;

$$w_c = Q/(V_c h_c) \tag{9}$$

$$\therefore \qquad S\cos\beta_c = Q/(V_c h_c) \tag{10}$$

and the critical angle is:

$$\beta_c = \cos^{-1}(q/(V_c h_c)) \tag{11}$$

This is the maximum angle that can be used. Any further increase in vane angle will block the flow, resulting in an increase in upstream depth.

<u>Critical vane speed</u>. The vane speed is also limited by critical flow conditions in the vane channels. For constant flow conditions and vane angles the relative velocity through the vane channels depends upon the vane speed U.
From Fig. 3b the vane speed U can be written as:

$$U = \sqrt{V_i^2 - (C_i\cos\alpha_i)^2} + C_i\sin\alpha_i \tag{12}$$

and for critical conditions:

$$V_i = V_c = \sqrt{gh_i} \tag{13}$$

$$\therefore \qquad U_c = \sqrt{gh_i - (C_i\cos\alpha_i)^2} + C_i\sin\alpha_i \tag{14}$$

For subcritical relative flow at the inlet to the vane channels $U_c > U$ and there is a maximum value of U where $U = U_c$.
With critical outlet conditions for the vane channels, the flow conditions upstream can be related to those downstream since the outlet depth h_o is the critical depth for the vane channel flow h_c and dependent only on q. However, for conditions other than critical the inlet and outlet conditions must be related by application of the energy and continuity equations to the relative flow through the vane channels.

<u>Relative flow through the vane channels</u>. Ideal flow relative to the vane channels is represented by Fig. 4. The energy equation for this flow, at the inlet and outlet, can be written as:

$$E = V_i^2/2g + h_i = V_o^2/2g + h_o \tag{15}$$

By the continuity equation:

$$\left.\begin{aligned} Q &= V_i\, h_i\, S \cos\beta_i = V_o h_o S \cos\beta_o \\ \therefore\quad q &= V_i\, h_i \cos\beta_i = V_o\, h_o \cos\beta_o \end{aligned}\right\} \tag{16}$$

and $$V_i = q/(h_i \cos\beta_i) \quad ; V_o = q/(h_o \cos\beta_o) \tag{17}$$

Substitute for V_i and V_o in the energy equation (15) gives:

$$E = 1/2g\left(\frac{q}{h_i \cos\beta_i}\right)^2 + h_i = 1/2g\left(\frac{q}{h_o \cos\beta_o}\right)^2 + h_o \tag{18}$$

These can be written as:

$$h_i^3 - Eh_i^2 + k_i = 0 \quad ; \quad h_o^3 - Eh_o^2 + k_o = 0 \tag{19}$$

where $$k_i = 1/2g\left(\frac{q}{\cos\beta_i}\right)^2 \text{ and } k_o = 1/2g\left(\frac{q}{\cos\beta_o}\right)^2 \tag{20}$$

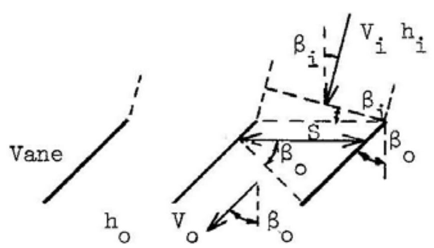

Fig. 4 Vane channel flow

These equations are of the third degree and have three real roots of which one is negative and hence not relevant to the present flow situation. The two positive roots correspond to two different depths of flow and two different corresponding velocities.

These two sets of values correspond to supercritical flow (large velocity, small depth) and subcritical flow (large depth, small velocity). This is discussed in reference [5].

To determine h_o for given values of E and k_o, equation (19) (for outlet conditions) is solved using Newton's numerical method [6] by writing

$$f(h) = h^3 - Eh^2 + k_o \qquad (21)$$

$$\frac{d\,f(h)}{dh} = f'(h) = 3h^2 - 2Eh \qquad (22)$$

If a value h_1 is substituted in these equations then a value h_2 closer to the solution than h_1 is given by:

$$h_2 = h_1 - \frac{f(h_1)}{f'(h_1)} \qquad (23)$$

Substitution of the new value of h_2 for h_1 gives convergence on the root of the equation, ie. the value of h_o.

Once the value of h_o is known, then, with β_o at some specified angle, the value for V_o can be determined from equation (17), enabling the velocity diagrams for the upstream and downstream flow to be drawn.

UPSTREAM AND DOWNSTREAM FLOW CONDITIONS

The velocity diagrams representing the ideal flow conditions upstream and downstream of the vanes for the upstream vanes (stage 1), and the downstream vanes (stage 2), are shown in Fig.5 together with a representation of the flow depth through the stages. These diagrams are drawn for subcritical flow conditions with the stream wise component of velocity increasing, corresponding to a decrease in flow depth. For convergent flow through the vane passages the relative velocity V_o cannot exceed the critical velocity V_c and hence C_o is always less than the critical velocity downstream. Consequently, the outlet depth (and hence energy) is greater than the critical minimum value. This constitutes an energy loss to the turbine.

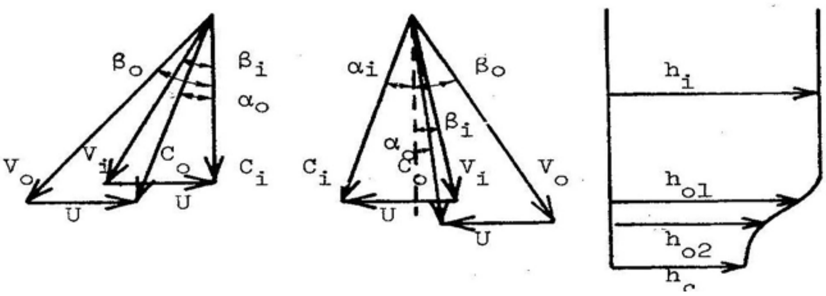

Upstream (stage 1) | Downstream (stage 2) | Flow depth

Fig. 5 Flow velocity diagrams and depth

Relationships and sign convention. The outlet flow conditions are expressed in relation to the inlet flow conditions using the sign convention of positive flow angles for flows with transverse components in the direction of U . The relationship for stage 1 and stage 2 flow conditions can be written as:

Stage 1 conditions:

$$\beta_i = -\tan^{-1}\left(\frac{U}{C_i}\right) \quad ; \quad V_i = \frac{C_i}{\cos\beta_i} \tag{24}$$

$$\alpha_o = \tan^{-1}\left(\frac{V_o \sin\beta_o + U}{V_o \cos\beta_o}\right) \quad ; \quad C_o = V_o \frac{\cos\beta_o}{\cos\alpha_o} \tag{25}$$

Stage 2 conditions:

$$C_i = C_o\,\text{(stage 1)} \quad ; \quad \alpha_i = -\alpha_o\,\text{(stage 1)} \tag{26}$$

$$\beta_i = \tan^{-1}\left(\frac{C_i \sin\alpha_i - U}{C_i \cos\alpha_i}\right) \quad ; \quad V_i = C_i \frac{\cos\alpha_i}{\cos\beta_i} \tag{27}$$

$$\alpha_o = \tan^{-1}\left(\frac{V_o \sin\beta_o + U}{V_o \cos\beta_o}\right) \quad ; \quad C_o = V_o \frac{\cos\beta_o}{\cos\alpha_o} \tag{28}$$

From these expressions the energy transfer to the vanes can be determined.

ENERGY TRANSFER

The energy transfer per unit mass flow for each stage can be expressed by the Euler equation as:

$$E = \frac{U}{g}(C_{ui} - C_{uo}) \tag{29}$$

or in terms of vane angles and relative velocities as:

$$E = \frac{U}{g}(V_i \sin\beta_i - V_o \sin\beta_o) \tag{30}$$

For the stage 1 vanes, $V_i \sin\beta_i = -U$ and hence:

$$E = -\frac{U}{g}(U + V_o \sin\beta_o) \tag{31}$$

For maximum energy transfer the magnitude of the term $V_o \sin\beta_o$ should be as large as possible (β_o is always negative). This will be the case if the outlet flow is critical with $V_o = V_c$ and $\beta_o = \beta_c$, ie:

$$E_{\max} = -\frac{U}{g}(U + V_c \sin\beta_c) \tag{32}$$

For critical flow conditions the stage 1 channel flow energy can be expressed as:

$$E_c = \frac{3}{2}h_c = \frac{V_i^2}{2g} + h_i = \frac{U^2 + C_i^2}{2g} + h_i \tag{33}$$

ie,
$$E_c = \frac{U^2}{2g} + E_i \tag{34}$$

and
$$\left.\begin{aligned} h_c &= \frac{U^2}{3g} + \frac{2}{3}E_i\,;\; V_c^2 = \frac{U^2}{3} + \frac{2gE_i}{3} \\ \beta_c &= -\cos^{-1}\left(\frac{q}{V_c h_c}\right) \end{aligned}\right\} \tag{35}$$

For optimum conditions the outlet flow from stage 2 should be as close as possible to the downstream conditions for minimum energy flow, ie. $h_o = h_c$, $V_o = V_c$, and $\beta_o = \beta_c$ and $\alpha_o = 0$. To obtain these optimum conditions requires selection of the appropriate upstream conditions by trail and error.

Power output. This is the rate of energy transfer and hence for each stage:

$$P = \rho q U\,(V_i \sin\beta_i - V_o \sin\beta_o) \qquad (36)$$

For maximum power output the energy transfer should be a maximum and hence outlet conditions critical.

FORCE ON THE VANES

The force on the vanes is dependent on the pressure drop across the vanes and the rate of change of momentum of the flow through the vanes. In the direction transverse to the upstream flow the pressure remains constant and the force is given by:

$$F_t = \rho q\,(V_i \sin\beta_i - V_o \sin\beta_o) \qquad (37)$$

For the stage 1 vanes, when $U = 0$, from Fig. 5, $V_i = C_i$, $V_o = C_o$, $\beta_i = 0$ and $\beta_o = \alpha_o$,

therefore $$F_{t1} = -\rho q C_o \sin\alpha_o \qquad (38)$$

From the stage 2 vanes, when $U = 0$, $V_i = C_i$ and $\beta_i = \alpha_i$, hence from (26), $V_i = C_{o1}$ and $\beta_i = -\alpha_{o1}$, therefore from (37):

$$F_{t2} = \rho q(C_{o1} \sin(-\alpha_{o1}) - V_{o2} \sin\beta_{o2})$$

$$= F_{t1} - \rho q V_{o2} \sin\beta_{o2} \qquad (39)$$

The maximum force on the vanes will be when deflection is at the critical angle α_{oc} and outlet conditions are critical. In this case, from (38):

$$F_{t1\max} = -\rho q C_{oc} \sin\alpha_{oc} \qquad (40)$$

giving critical inlet conditions to stage 2.

ie. $$V_{i2} = C_{oc1} \;;\quad \beta_{i2} = -\alpha_{oc1} \qquad (41)$$

Hence for maximum force on the stage 2 vanes,

$$V_{o2} = V_{i2} = C_{oc1} \;;\; \beta_{o2} = -\beta_{i2} = \alpha_{oc1} \qquad (42)$$

therefore $$F_{t2\max} = 2F_{t1\max} \qquad (43)$$

EXPERIMENTAL TESTS

Test rig details. As a preliminary evaluation of the validity of the theory, a test rig consisting of a cascade of six vanes was made and suspended in a channel flow to obtain experimental values for F_t at different vane angles and depths. Details of the test rig arrangement are given in Fig. 6.

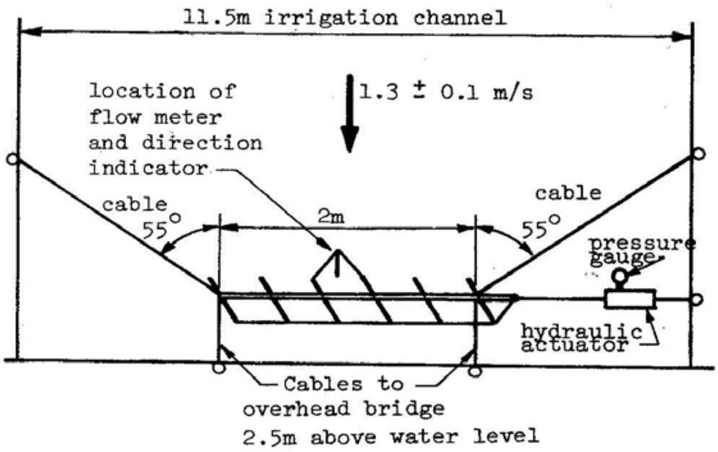

Fig. 6 Details of test rig arrangement

The vanes were set in the rig at specified angles for each test and vane depth was adjusted by vertical cables from the overhead bridge. The transverse force was measured by a hydraulic actuator (fitted with a pressure gauge) which was secured to the right bank of the channel.

The vanes of the test rig were made from 12mm plywood 450mm wide by 900mm deep with a 40° bevel on the downstream side of the leading edge. The top and bottom ends were stiffened with 20mm x 20mm angle steel attached to the upstream side of the vanes. This angle was bolted to the test rig frame at the 1/3 chord position with a vane spacing of 400mm. The trailing edges of the vanes were tied together at top and bottom with two steel strips which could be locked at different positions to give a range of vane angle settings.

Test measurements and accuracy. Flow velocity was measured with a propeller type flow meter positioned centrally 50mm upstream of the vanes and 250mm above the bottom level of the vanes. This meter had an accuracy of ± 0.05 m/s. The measured flow velocity was 1.3 ± 0.05 m/s so true flow conditions were taken as 1.3 ± 0.1 m/s. The alignment of the test rig to the channel flow was indicated by a 260mm wide plate fitted in place of the flow meter and pivoted at its leading edge with its trailing edge 50mm upstream of the vanes. Alignment was measured to be $4^\circ \pm 1^\circ$ over the range of tests and flow direction fluctuated $\pm 2^\circ$. Consequently the actual vane angles to the flow for the four settings were $14^\circ \pm 3^\circ$, $24^\circ \pm 3^\circ$, $34^\circ \pm 3^\circ$, and $39^\circ \pm 3^\circ$.

The transverse load was measured at each vane angle setting for vane depths of 400mm, 600mm, and 800mm. The bow wave in front of the vanes made it difficult to determine these depths to less than ± 50mm accuracy. Piston friction in the hydraulic actuator limited the load measurement accuracy to ± 250N.

Since the vanes were mounted at the 1/3 chord position it was assumed that moments about the vanes due to the load force would be small and therefore, since the rig and cables were symmetrical, there would be little difference in cable tensions to effect the load measurements.

Six vanes were used in the cascade to reduce the significance of the effect of the different flow conditions at each end. However, to be more certain about this effect, further tests need to be made with different numbers of vanes.

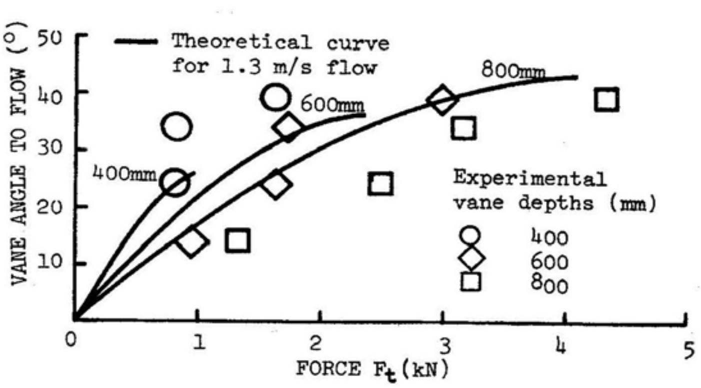

Fig. 7 Theoretical and experimental values for the force on a cascade of 6 vanes at 0.4m spacing in a 1.3m/s flow (experimental error: force ± 250N, angle ± 3 degrees, : flow ± 0.1m/s, vane depth ± 50mm)

RESULTS AND DISCUSSION

The test results are plotted in Fig. 7 together with values predicted by the theory for vane depths h_i of 400, 600 and 800mm, a flow $C = V_i = 1.3$ m/s and $\rho = 1000$ kg/m^3 (using equations 2, 15, 17, 19 and 38) for vane angles β_o from zero up to the critical vane angle β_c. At greater vane angles the theory predicts choked flow with a consequent reduction in flow and decrease in force, or alternatively an increase in inlet depth to maintain the same flow. The continuing increase in force at vane angles above the critical, observed in the experimental results could be partly due to an increase in inlet depth which was difficult to maintain accurately. This effect would be more significant at the lower vane depths and this tends to agree with the results. Entrainment of flow into the channel from the mainstream flow below the vanes could also be contributing to the deviation from the theory.

The experimental values for the 600 and 800mm depths tend to be higher than the

theoretical values, especially at the higher vane angles. This deviation is possibly due to the deviation from ideal flow conditions in the channels, and around the end vanes of the cascade, due to boundary layer growth, separation, and uneven velocity distribution across the flow, which would all tend to reduce the effective flow area, resulting in higher outlet velocities and hence greater vane loads at subcritical flow conditions.
From observation of the flow during the tests it is felt that with improved vane design, vane channel flows closer to the ideal flow conditions could be achieved, resulting in better agreement with the theoretical predictions.
Since the channel flows analysed in the theory are relative flows it seems reasonable to expect that conditions with different values of vane speed could be simulated by a stationary cascade with different inlet flow velocities and alignment angles to the flow. If this is so, then the general agreement with the theory shown by the present test results suggests that predictions based on the theory for a linear turbine running at various vane speeds would also be valid.

THEORETICAL PERFORMANCE PREDICTIONS

Future plans are to construct a full size linear turbine, with a vane depth of 800mm, to operate in a channel flow similar to that used for the vane cascade tests (ie. 1.3m/s flow). To gain a rough estimate of the performance and design criteria for this turbine a computer program, based on the theory of this paper, was run with vane outlet angles at the critical values ($\beta_o = \beta_c$) and varying values of vane speed. The results are given in Fig. 8. Force per meter was calculated from equation (37) using critical values for V_o and β_o determined from equation (35). Power per meter was calculated from equation (36). At $U = 0$, for the conditions in Fig. 8, the theoretical value for β_c from equation (35) is 43 degrees, and since this condition is close to the test result in Fig. 7 for the vanes at 800mm depth and 39 ± 3 degrees vane setting, this value has been converted to force per meter and plotted in Fig. 8 for reference.
The force per meter for stage 2 is shown in Fig. 8 to be twice that of stage 1 as predicted by equation (43) and this drops to the same value as for stage 1 at about U = 0.9m/s where the total power is at a maximum of 1.68kW/m.
The upper limit of U corresponds to the critical value of 2.48m/s determined from equation (14).

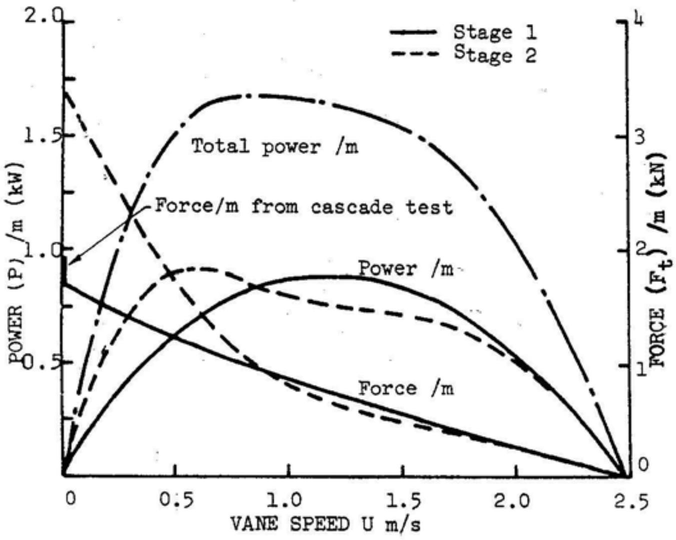

Fig. 8 Theoretical values foe a 2 stage linear turbine with critical flow conditions at stage 1 and stage 2 outlets and upstream flow 1.3m/s and 800mm deep

CONCLUSIONS

Use of the equations for open channel flow and the Euler turbine equations enables construction of a basic mathematical model for prediction of the flow conditions through an open channel flow linear turbine.

The general agreement of theoretical predictions, for the force on a vane cascade transverse to the upstream flow, with experimental results, suggests that the theory could be useful in determining design criteria for a linear turbine.

Theoretical calculations for a linear turbine in a flow of 1.3m/s and 800mm deep predict a maximum power output of 1.68kW per meter transverse to the flow.

Further tests are required with a variety of cascade arrangements and vane shapes, and also with linear turbines operating under various flow conditions, before the theory can be considered sound.

ACKNOWLEDGEMENTS

The authors would like to thank Messrs. J. Shootsu, T. Yamada, and H. Ohma of the Fukui Institute of Technology Mechanical Engineering Department for their invaluable assistance in carrying out the experimental tests.

REFERENCES

1. Powe, R. E., “A wind energy conversion system based on the tracked vehicle airfoil

concept," BHRA Fluid Engineering Symposium on Wind Energy Systems, Cambridge, Sept. 1976, paper B3 pp39-53.
2. "Lifting foils tap power in a California irrigation canal," an article about application of the Schneider Lift Translator system, Popular Science, January 1982.
3. "Wind powered pulleys," Popular Science, February 1982, p.85.
4. Schaum's Outline Series, Fluid Mechanics and Hydraulics, McGraw-Hill, 1977.
5. Kaufmann, W., Fluid Mechanics, McGraw-Hill, New York, 1963, pp131-132.
6. Stanton, R. G., Numerical Methods for Science and Engineering, Tokyo, Maruzen, 1961, p84.